# Novel $\beta$-Cyclodextrin-Based Heptavalent Glycyrrhetinic Acid Conjugates: Synthesis, Characterization, and Anti-Influenza Activity

Shuobin Liang, Xinyuan Ma, Man Li, Yanliang Yi, Qianqian Gao, Yongmin Zhang, Lihe Zhang, Demin Zhou, Sulong Xiao

# Novel *β*-cyclodextrin-based heptavalent glycyrrhetinic acid conjugates: Synthesis, characterization and anti-influenza activity

Shuobin Liang[a,1], Xinyuan Ma[a,1], Man Li[a], Yanliang Yi[a], Qianqian Gao[a], Yongmin Zhang[d], Lihe Zhang[a], Demin Zhou[a,b,c], Sulong Xiao[a,*]

[a] *State Key Laboratory of Natural and Biomimetic Drugs, School of Pharmaceutical Sciences, Peking University, Beijing 100191, China*

[b] *Institute of Chemical Biology, Shenzhen Bay Laboratory, Shenzhen 518132, China*

[c] *Ningbo Institute of Marine Medicine, Peking University, Ningbo 315010, China*

[d] *Sorbonne Université, Institut Parisien de Chimie Moléculaire, CNRS UMR 8232, 4 place Jussieu, 75005 Paris, France*

[1] These authors contributed equally to this work.

[*]Corresponding author. *E-mail address*: slxiao@bjmu.edu.cn

**Abstract**

In our continuing efforts toward the design of novel pentacyclic triterpene derivatives as potential anti-influenza virus entry inhibitors, a series of homogeneous heptavalent glycyrrhetinic acid derivatives based on $\beta$-cyclodextrin scaffold were designed and synthesized by click chemistry. The structure was unambiguous characterized by NMR, IR, and MALDI-TOF-MS measurements. Seven conjugates showed sufficient inhibitory activity against influenza virus infection based on cytopathic effect reduction assay with $IC_{50}$ values in the micromolar range. The interactions of conjugate **37**, the most potent compound ($IC_{50}$ = 2.86 $\mu$M, $CC_{50}$ > 100 $\mu$M), with influenza virus were investigated using hemagglutination inhibition assay. Moreover, surface plasmon resonance assay further confirmed that compound **37** bound to influenza HA protein specifically with a dissociation constant of $5.15 \times 10^{-7}$ M. Our results suggest the promising role of $\beta$-cyclodextrin as scaffold for preparing a variety of multivalent compounds as influenza entry inhibitors.

**Keywords**: Glycyrrhetinic acid; $\beta$-cyclodextrin; influenza virus; multivalency; hemagglutinin

## 1. INTRODUCTION

Influenza A virus is a highly contagious respiratory pathogen that can cause seasonal epidemics and irregular pandemics due to its rapid transmission and frequent genetic alteration (Neumann et al., 2009; Lagacé-Wiens et al., 2010). The structure of the viruses consists of a lipid envelope that is generated from the host cell, to which two dominant membrane proteins hemagglutinin (HA) (80%, ~300 copies of trimer) and neuraminidase (NA) (17%, ~50 copies of tetramer) are anchored (Leser et al., 2005). Based on the antigenicity of HA and NA, they can be classified into different subtypes. To date, 18 major antigenic variants of HA and 11 antigenic variants of NA have been recognized, which are found in numerous combinations. In addition, newly mutated forms of the influenza virus appear every year. The current available options to combat influenza A viral infections include the prophylactic, yearly reformulated vaccines and two classes of anti-influenza drugs (the M2 ion-channel inhibitors and the NA inhibitors) (Das, 2012). Since the vaccines that are available now offer a very limited breadth of protection (van Dongen et al., 2019), the antiviral drugs are still the first line of protection to treat acute influenza infection. Unfortunately, all circulating influenza A viral strains appear to be resistant to the M2 ion-channel inhibitors. Recently, the continually emerging of resistant virus against NA inhibitors has been also reported (Hurt et al., 2006; van der Vries et al., 2010; Hurt, 2014). For these reasons, novel anti-influenza viral agents with new targets and mechanisms of action are urgently required to overcome the rapid emergence of drug resistance (Heo, 2018; van Dongen et al., 2019).

In the first step of infection, the virion adheres to the host cell surface through the binding of HA to sialic acid-terminated carbohydrates present on the cell membranes (Mammen et al., 1998; Skehel et al., 2000). Therefore, HA plays a pivotal role in virus entry, making it a potential target for antiviral intervention. HA is a homotrimeric integral membrane glycoprotein, which has ca. 300-400 copies on the viral surface (Mammen et al., 1998). The monovalent interaction between HA and sialic acid is mediated essentially by hydrogen bonds, and the dissociation constant of them shows a relative weak binding ($K_D$ ~ 2 mM) (Sauter et al., 1989). Therefore, a multitude of HA is involved in order to increase the overall strength of the interaction between the virus and the host cell. The binding between multiple pairs of HA trimer and sialic acid ligand increases substantially as characterized by a multivalent affinity constant of estimated $10^{13}$ $M^{-1}$ (Mammen et al., 1998). This process provides important clues for the design of efficient multivalent ligands to mimic the binding of HA to sialic acid to block the viral protein-host receptor interactions (Lu et al., 2019). Over the past few years, many efforts have been made for the design and synthesis of carbohydrate-based multivalent HA binders, including polymers, dendrimers, nanoparticles and so on, serving as potent influenza A virus inhibitors (Chaudhary et al., 2019; Lu et al., 2019).

*β*-Cyclodextrin (*β*-CD) is a torus shaped cyclic oligosaccharide consisting of seven (*α*-1,4)-linked D-glucopyranose units and it is well-known for their ability to form inclusion complexes with a broad variety of organic and inorganic compounds (Crini, 2014). It is widely

used in pharmaceutical formulations to enhance the solubility of poorly soluble drugs, increase drugs permeability through biological membranes and improve the bioavailability of drugs (Jansook et al., 2018). The unique steric accessibility and acidity of the three types of hydroxyls in $\beta$-CD have been taken into account to conceive efficient position-selective and face-selective chemical functionalization methodologies (Khan et al., 1998). It has been shown to serve as a multivalent scaffold in the design of glycoconjugates (Martinez et al., 2013), glycoclusters (Gomez-Garcia et al., 2005; Gomez-Garcia et al., 2012), glycodendrimers (Ortega-Caballero et al., 2001; Vargas-Berenguel et al., 2002) and star polymers (Zhang et al., 2012; Gonzalez-Gaitano et al., 2017). In addition, target-specific multivalent drug delivery systems have shown significant improvement of anti-tumor drugs delivery and hence antitumor efficacy and prevention of clinical multi-drug resistance (Kim et al., 2017; Zhou et al., 2019).

In spite of the progress, the design of multivalent ligands with optimized biological properties still remains a challenge considering the complexity of the multivalent ligand-receptor interactions (Lepage et al., 2015). Glycyrrhizic acid (also known as glycyrrhizin, **1**) (Fig. 1), an oleanane-type pentacyclic triterpene saponin, is the primary bioactive constituent of the roots and rhizomes of *Glycyrrhiza glabra* (licorice) which is employed as an herbal medicine in both Western and Eastern countries (Fiore et al., 2005; Asl et al., 2008). Compound **1** and its aglycone, glycyrrhetinic acid (GA, **2**), have been reported to possess antitumor, anti-inflammatory and other pharmacological activities (Yang et al., 2015; Hussain et al., 2018). In a notable example, Lallemand *et al.* have reported that compound **3**, with a 2-(3-(3,5-bis(trifluoromethyl)phenyl)ureido)ethyl group at C-30 of **2**, shows strong antitumor activity with $IC_{50}$ in signal-digit micromolarity in a panel of eight cancer cell lines (Lallemand et al., 2011). Recently, attention to GAs has been greatly increased due to their broad spectrum of antiviral activities, such as anti-hepatitis B virus (HBV) (Wang et al., 2012), anti-Epstein-Barr virus (EBV) (Lin et al., 2008), anti-rotavirus (Hardy et al., 2012), anti-influenza virus (Stanetty et al., 2012), anti-herpes simplex virus (HSV) (Zigolo et al., 2018), etc. 3-Thioglucuronide derivative **4** and several C-30 ester derivatives, such as 4-(trifluoromethyl) benzyl ester (**5**), 4-iodobenzyl ester (**6**) and 4-nitrobenzyl ester (**7**), show promising antiviral activity (Stanetty et al., 2012; Wang et al., 2012). In our previous study, a series of monovalent $\beta$-CD-GA conjugates have been synthesized and several conjugates show weak antiviral activity at high concentration (~50 $\mu$M) (Liang et al., 2019). As a natural step in our efforts towards the design of new pentacyclic triterpene conjugates with antiviral activity (Yu et al., 2014; Xiao et al., 2016; Si et al., 2018), we described herein the design and synthesis of a series of heptavalent GA functionalized $\beta$-CD conjugates and evaluated their *in vitro* anti-influenza activity.

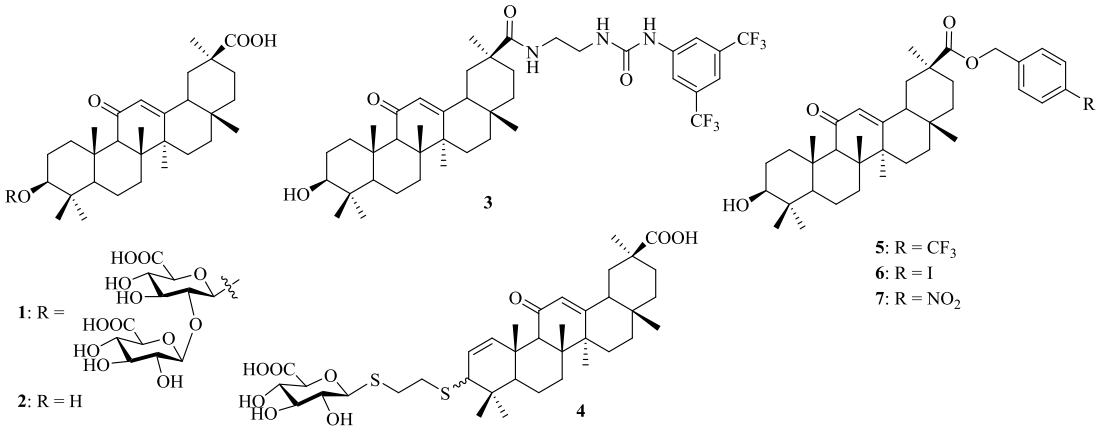


**Figure 1.** Chemical structures of glycyrrhizic acid (**1**), GA (**2**) and its derivatives (**3**-**7**).

## 2. MATERIALS AND METHODS

### *2.1 Materials*

GA was kindly supplied by Nanjing Zelang Medical Technology Co., Ltd. (China). *β*-CD, *O*-(benzotriazol-1-yl)-*N*,*N*,*N*′,*N*′-tetramethyluroniumtetrafluoroborate (TBTU), *N*,*N*-Diisopropylethylamine (DIPEA), iodine, triphenylphosphine, sodium azide, 4-dimethylaminopyridine (DMAP), cupric sulfate were purchased from Shanghai Aladdin Bio-ChemCo. Ltd. (China). Sodium ascorbate, sodium methoxide, 5-hexyn-1-amine and 4-ethynylaniline were supplied by Shanghai Energy Chemicals (China). Silica gel 60 (200-300 mesh) was provided by Qingdao Haiyang Chemical Co., Ltd. (China). Sodium carbonate, *N*,*N*-dimethylformamide, tetrahydrofuran, methanol, pyridine, acetic anhydride as well as all other chemicals and reagents used were of analytical grade and purchased from Sinopharm Chemical Reagent Co., Ltd. (China) and used throughout this research without further purification.

Thin-layer chromatography (TLC) was conducted on a pre-coated silica gel 60 $F_{254}$ plate (E. Merck, Darmstadt, Germany) and eluted with a mixture of methanol/dichloromethane (15:1~10:1) for per-*O*-acetyl-*β*-CD-GA conjugates or methanol for the deacetylated *β*-CD-GA conjugates. For spot detection, the plates were immersed in a yellow solution of $Ce(NH_4)_2(NO_3)_6$ (0.5 g)/$(NH_4)_6Mo_7O_{24}{\cdot}4H_2O$ (24.0 g)/6% $H_2SO_4$ (500 mL). The plate was heated by hot gun in order to visualize the spots. FT-IR spectra were obtained using a Nicolet Nexus 470 FTIR spectrometer (Thermo Electron Scientific Instruments LLC, USA). MALDI-TOF mass spectra were obtained on an AB Sciex TOF/TOF$^{TM}$ 72115 spectrometer using methanol or chloroform as solvents and *α*-cyano-4-hydroxy-cinnamic acid (HCCA) as matrix. NMR spectra were recorded on a Bruker DRX 400 or DRX 600 spectrometer at ambient temperature.

Madin-Darby canine kidney (MDCK) cells were donated by Crown Bioscience Inc. (USA). Dulbecco's Modified Eagle Medium (DMEM) was purchased from Gibco BRL, Inc. (USA). CellTiter-Glo® reagent was purchased from Promega Corp Inc. (USA). Recombinant influenza HA was purchased from Sino Biological Inc. (China). Deionized double-distilled water was used

throughout the biological study. Surface plasmon resonance (SPR) assay was analyzed using the Biacore 8k system (GE Healthcare, Uppsala, Sweden).

*2.2 Synthesis of heptavalent β-CD-GA conjugates*

Heptakis (2,3-di-*O*-acetyl-6-deoxy-6-azide-)-*β*-CD **11** was prepared in a three-step procedure as previously reported (Gadelle et al., 1991). The GA intermediate **12** was synthesized based on the method of Schwarz *et al*. with minor modifications (Schwarz et al., 2014). The terminal alkynyl substituted amines **13-16** were prepared as previously described (Murelli et al., 2009; Zhang et al., 2010; Tran et al., 2013; Sanhueza et al., 2017). Alkynyl-functionalized GA intermediates **17-20** and **30-32** were synthesized as previously described (Liang et al., 2019). Heptavalent GA functionalized *β*-CD conjugates were synthesized through a two-step process involving the copper-catalyzed alkyne–azide cycloaddition reaction (CuAAC) under microwaves (step 1) and de-*O*-acetylation reaction under Zemblén conditions (step 2).

*2.2.1 General procedure A for the click reaction (step 1)*

To a solution of heptakis (2,3-di-*O*-acetyl-6-deoxy-6-azide-)-*β*-CD **11** (189.8 mg, 0.10 mmol) and alkynyl-functionalized GA derivatives (0.84 mmol) in 50% of THF and $H_2O$ (5 mL) was added $CuSO_4$ (15.7 mg, 0.10 mmol) and sodium ascorbate (30.7 mg, 0.15 mmol). The resulting solution was heated in a microwave reactor at 100$^{o}$C until the azide was completely consumed (typically about 1 h) as determined by TLC. Then the reaction mixture was extracted with $CH_2Cl_2$ (10 mL × 3). The $CH_2Cl_2$ fraction was dried over $Na_2SO_4$, filtered, evaporated, and purified by silica gel column chromatography using $CH_2Cl_2$/$CH_3OH$ (15:1~10:1 v/v) as eluent to give the acetylated intermediates as a white foam.

*2.2.2 General procedure B for the deacetylation reaction (step 2)*

The multivalent GA functionalized per-*O*-acetylated *β*-CD conjugates were dissolved in dry methanol (5 mL per 100 mg of compound), and a solution of sodium methoxide (30% in methanol, 0.1 eq per mol of acetate) was added. The solution was stirred (180 rpm) at room temperature for 4~6 h in a $N_2$ atmosphere. After completion (TLC), the reaction mixture was neutralized with Amberlite IR-120 ($H^+$) ion exchange resin, then filtered and concentrated. The crude product was purified by RP column chromatography using $CH_3OH$ as eluent to give the final products in 73-95% yields.

The $^{1}$H and $^{13}$C NMR and ESI-HRMS or MALDI-TOF MS data of the synthesized new compounds **21-28** and **33-38** are available in supporting information (Supplementary Data, S6-S14).

*2.3 FT-IR analysis*

FT-IR spectra of the heptavalent *β*-CD-GA conjugates as well as their parent compounds **11** and **17** were obtained using a Nicolet Nexus 470 FTIR spectrometer (Thermo Electron Scientific Instruments LLC, USA) over a scanning range 500-4,000 $cm^{-1}$. In addition, 1.0 mg of different samples was mixed with KBr pellets.

*2.4 NMR study*

$^{1}H$ and $^{13}C$ NMR spectra of GA derivatives **17**-**20** and **29**-**32** were acquired on a Bruker DRX 400 MHz spectrometer. $^{1}H$ NMR, $^{13}C$ NMR, $^{1}H$-$^{1}H$ COSY NMR and $^{1}H$-$^{13}C$ HSQC NMR spectra of $\beta$-CD-GA conjugates **21**-**28** and **33**-**38** were acquired on a Bruker DRX 600 MHz spectrometer. Sample solutions were prepared with $CDCl_3$ or $CDCl_3/CD_3OD$ (2:1) as solvent. $CDCl_3$ or $CD_3OD$ were also employed as reference: proton ($\delta$ 7.26 ppm) and carbon ($\delta$ 77.00 ppm) for $CDCl_3$, proton ($\delta$ 3.31 ppm) and carbon ($\delta$ 49.00 ppm) for $CD_3OD$. Detection temperature was set at 25 °C.

*2.5 Cell culture and viruses*

MDCK cells were donated by Crown Bioscience Inc. (USA) and grown in DMEM supplemented with 10% (v/v) fetal bovine serum (FBS) (PAA Laboratories, Linz Austria) at 37 °C under 5% $CO_2$. The A/WSN/33 (H1N1) influenza virus used in this study was artificially generated from the 12-plasmid influenza virus rescue system.

*2.6 Cytotoxicity assay*

Cell viability assays were performed using CellTiter-Glo® reagent following the manufacturer's instructions. Briefly, the cells ($1\times10^4$ per well) were seeded into 96-well tissue culture plates and incubated for 16 h at 37 °C with 5 % $CO_2$ to allow the cells to adhere to the surface of the wells. The culture medium was then replaced with fresh medium containing compound or paclitaxel (PTX) at 10 and 25 $\mu$M in triplicate, and the negative control wells contained the equivalent volume of medium with 1% DMSO, after which they were incubated for 48 h at 37 °C with 5% $CO_2$. CellTiter-Glo® reagent was added, and the plates were read using a Tecan Infinite M2000 PRO™ plate reader.

*2.7 Cytopathic effect (CPE) reduction assay*

MDCK cells ($1 \times 10^4$ per well) were seeded into 96-well plates, incubated at 37 °C with 5 % $CO_2$ for 24 h and infected with influenza virus (MOI = 0.1). Cells were suspended in DMEM supplemented with 1% FBS, containing different concentrations test compound or Oseltamivir (OSV) and 2 $\mu$g/mL TPCK-treated trypsin, and a final DMSO concentration of 1% was added in each well. After 48 h of incubation at 37 °C with 5 % $CO_2$, CellTiter-Glo® reagent (Promega Corp., Madison, WI, USA) was added, and the cells were assessed with the CellTiter-Glo® assay according to the manufacturer's instructions.

*2.8 Hemagglutination inhibition (HI) assay*

HI assay was performed as described previously (Yu et al., 2014). Briefly, compound from a 2-fold serial dilution in saline was mixed with an equal volume of influenza virus (2 HA units) in the V-bottomed 96-well microplates. Subsequently, 50 $\mu$L of freshly prepared chicken red blood cells (cRBC) (1% v/v in saline) was added to each well. The mixture was incubated at room temperature for 30 min before observing cRBC aggregation on the plate.

*2.9 SPR assay*

Interactions between influenza HA and the compounds were analyzed using the Biacore 8k system (GE Healthcare, Uppsala, Sweden) at 25 °C. Recombinant influenza HA (Sino Biological Inc., Beijing, China) was immobilized on a sensor chip (CM5) using EDC and NHS for activation. Final HA immobilized levels were typically ~9,000 RU. Subsequently, compounds were injected as analytes at various concentrations, and PBS-T (10 mM phosphate buffer with 5% DMSO, 0.05% Tween, pH 7.4) was used as the running buffer. For binding studies, analytes were applied at corresponding concentrations in running buffer at a flow rate of 30 $\mu$L/min with a contact time of 60 s and a dissociation time of 180 s. Chip platforms were washed with running buffer and 50% DMSO. Data were analyzed with the Biacore insight evaluation software (version 1.05) by curve fitting using a binding model of 1:1.

## 3. RESULTS AND DISCUSSION

*3.1 Synthesis of heptavalent β-CD-GA conjugates*

As shown in Scheme 1, the synthetic strategy was based on coupling of alkynyl-functionalized Gas with heptaazide substituted *β*-CD via click chemistry. At first, oligo (ethylene glycols) (OEGs) were chosen as linkers to enhance and optimize the properties of conjugates. Various heterobifunctional OEGs with amine and alkynyl terminals **13-16** were synthesized as described previously (Murelli et al., 2009; Zhang et al., 2010; Tran et al., 2013; Sanhueza et al., 2017). The coupling of OEGs **13-16** with compound **12**, which obtained from commercially available GA **2** by activation of the carboxylic acid at C-30, was performed to provide the alkynyl-functionalized GAs **17-20**. Then **17-20** underwent a "click chemistry" reaction with heptakis (2,3-di-*O*-acetyl-6-deoxy-6-azide)-*β*-CD **11**, which was prepared from *β*-CD **8** in three steps using the conventional method as previously described (Gadelle et al., 1991; Ashton et al., 1996; Karginov et al., 2006) in the presence of copper sulfate and sodium ascorbate as reducing agent to give **21-24** with yields ranging from 54% to 88%. At last, the acetyl groups of multivalent conjugates **21-24** were removed under Zemblén conditions, followed by neutralization with $H^+$ resin to afford **25-28** in 73-86% yields.

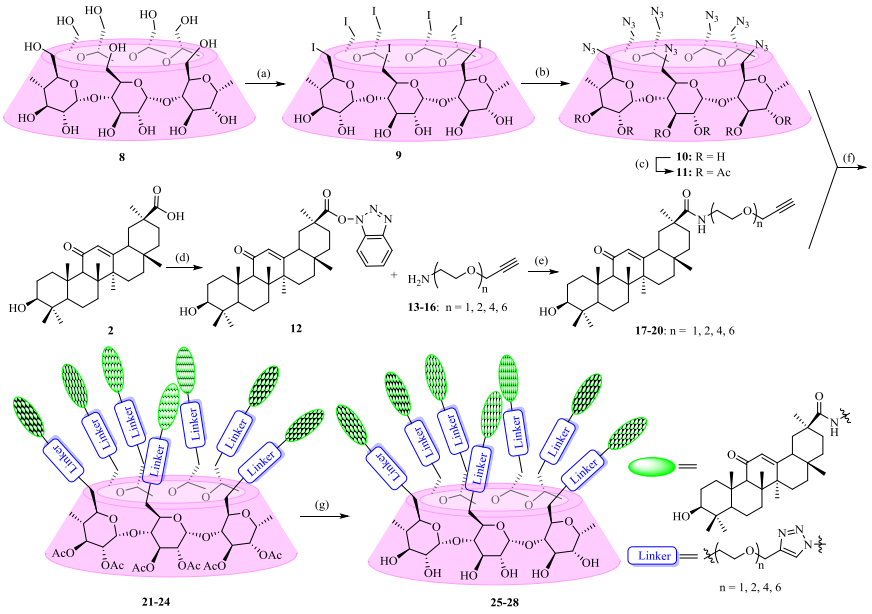

**Scheme 1.** Synthesis of heptavalent GA functionalized *β*-CD conjugates (**21-28**). Reagents and conditions: (a) $I_2$, $Ph_3P$, DMF, 80°C, 44%; (b) $NaN_3$, DMF, 60°C, 90% (c) Py, $Ac_2O$, DMAP, 92%; (d) TBTU, DIPEA, THF, 90%; (e) $Na_2CO_3$, DMF, 60°C, 46-82%; (f) Sodium ascorbate, $CuSO_4$, THF-$H_2O$ (1:1, v/v), 54-88%; (g) MeOH, MeONa, 73-86%.

To highlight the effect of the linkers on the anti-influenza virus activity, a parallel experiment was carried out to conjugate GA with *β*-CD moiety through an alkyl chain or a more rigidness chain, such as benzene ring or piperazine ring, rather than an OEG linker (Scheme 2). In a similar pathway, coupling of compounds **29**, **30** and **32** with heptaazide *β*-CD intermediate **11** was performed via click reaction, followed by de-*O*-acetylation under Zemplén conditions to give the corresponding conjugates **34**, **36** and **38**, respectively, as the final products.

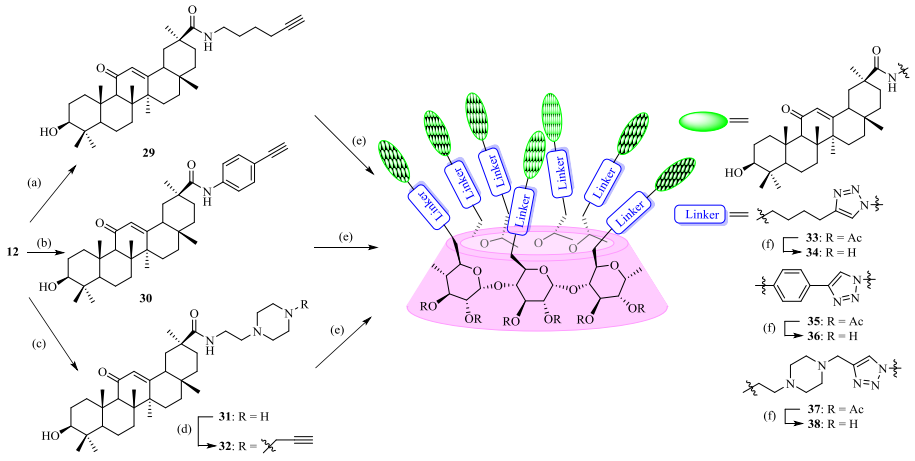

**Scheme 2.** Synthesis of heptavalent GA functionalized *β*-CD conjugates (**33-38**). Reagents and conditions: (a) 5-hexyn-1-amine, $Na_2CO_3$, DMF, 60°C, 90%; (b) 4-ethynylaniline, $Na_2CO_3$, DMF, 60°C, 30%; (c) 2-(piperazin-1-yl)ethan-1-amine, $Na_2CO_3$, DMF, 60°C, 45%; (d) propargyl bromide, $Na_2CO_3$, DMF, 60°C, 76%; (e) **11**, sodium ascorbate, $CuSO_4$, THF-$H_2O$ (1:1, v/v), 42-59%; (f) MeOH, MeONa, 90-95%.

*3.2 Structure characterization of heptavalent β-CD-GA conjugates*

The structures and symmetrical substitution of the heptavalent *β*-CD-GA conjugates **21-28** as well as their precursors **33–38** were characterized by IR, NMR and MALDI-TOFMS spectroscopy.

*3.2.1 FT-IR analysis*

The FTIR spectra of the all synthesized heptavalent *β*-CD-GA conjugates were recorded over the range of 400-4,000 $cm^{-1}$ in a Nicolet Nexus 470 FT-IR thermo-scientific spectrophotometer. The spectrum of *β*-CD intermediate **11** contained the characteristic absorption band for the spectrum with OH stretching at 3,386 $cm^{-1}$, CH stretching around 2,924 $cm^{-1}$ and CO stretching around 1,030 $cm^{-1}$ (Supplementary data Fig. S1). For GA (**2**), several vibration characteristics of the triterpenic moiety were present. The characteristic band attributed to the stretching vibration of the OH group at C3 was found at 3,443 $cm^{-1}$. And the bands at 2,930 and 2,870 $cm^{-1}$ were assigned to the stretching vibration of the aliphatic CH (Supplementary data Fig. S2). The spectra of these heptavalent *β*-CD-GA conjugates were very similar. In a typical example, Fig. 2 shows the IR spectra of the two intermediates **11**, **17** and their conjugate **21**. It was noteworthy that the strong absorption band located at 2,107$cm^{-1}$ in Fig. 2A and the weak absorption band located at 2,120 $cm^{-1}$ in Fig. 2B, which should be assigned to the stretching vibration of azide and terminal alkyne, respectively, were diminished in the spectrum of **21** (Fig. 2C). In addition, a few representative absorption bands ascribable to 1,2,3-triazole units were shown around 1,529, 1,455 and 1,047 $cm^{-1}$ (Rao et al., 1964).

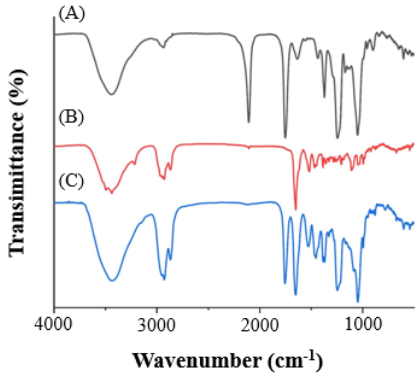


**Figure 2.** FTIR spectra of compounds **11** (A, black), **17** (B, red) and their conjugate **21** (C, blue). Spectra were acquired between 500 and 4,000 $cm^{-1}$.

*3.2.2 NMR and MALDI-TOF MS analysis*

Except for those signals of the linkers, the heptavalent conjugates were similar in their NMR spectra, and Fig. 3 represents the HSQC spectrum of conjugate **23** as an example. The low-field regions of the conjugate were relatively well resolved and fully assigned. In the aromatic region, the signal at $\delta$ 7.76 ppm was assigned to triazole-CH according to the $^{1}H$-$^{13}C$ correlation spectra, indicating that it was indeed connected by triazole linker. The assignment of NH proton at $\delta$ 6.31 ppm was confirmed as there was no correlation for NH by HSQC spectral analysis. The low-field

peak at $\delta$ 5.64 ppm, referring to 1H, was assigned to $H_{12}$, and one carbon appearing at $\delta$ 128.35 ppm should be assigned to $C_{12}$ of GA. With a $C_7$-symmetry in the molecule, compound **23** showed only one set of CD-$H_1$ signal appearing at 5.49 ppm and one CD-$C_1$ signal appearing at 96.29 ppm. Similar observation was also made for other proton and carbon signals of $\beta$-CD unit, and the chemical shift data are summarized in Table 1. As $C_b$ was connected with nitrogen rather than oxygen to which other carbons were bonded in tetraethylene glycol linker, the chemical shift of $C_b$ in $^{13}$C NMR was at the highest field (NH<u>C</u>$H_2$ *vs* O<u>C</u>$H_2$). In addition, as $C_a$ was connected with triazole, the chemical shift of $H_a$ in $^1$H NMR was at the lowest field among the eight -$OCH_2$- groups. The MALDI-TOF MS of compound **23** showed a sodium adduct ion $[M + Na]^+$ at *m/z* 6709.6 (Calcd. For $C_{357}H_{546}N_{28}NaO_{91}$, 6709.4), which also confirmed that it was a heptavalent conjugate.

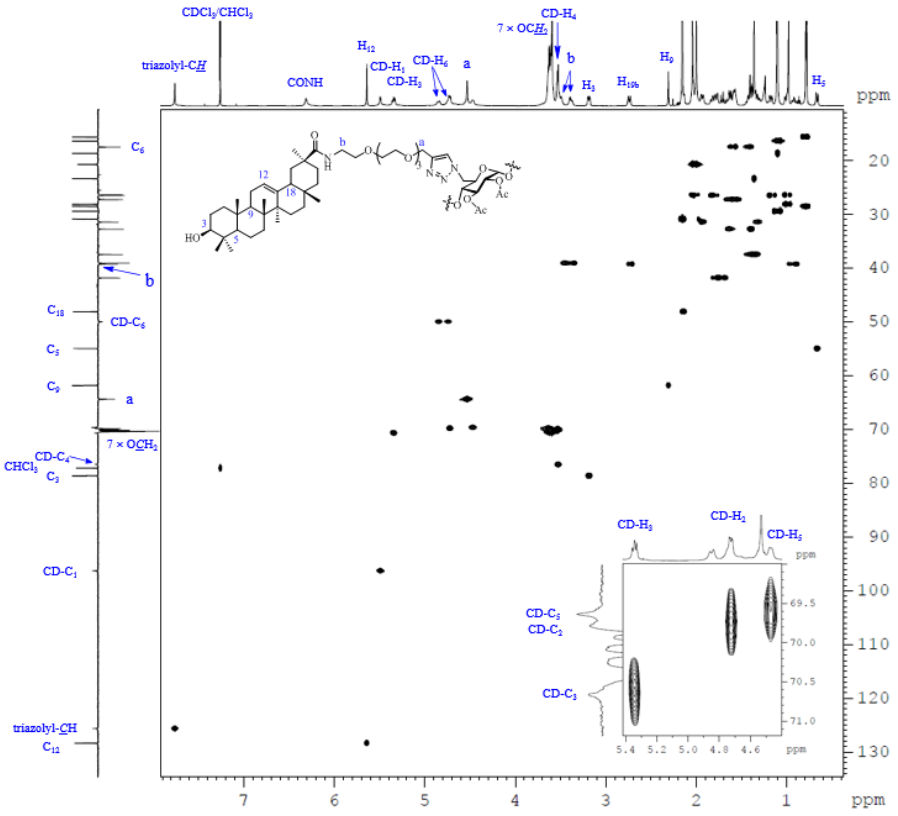


**Figure 3.** The 600 MHz HSQC spectrum of **23** recorded in $CDCl_3$ at 298 K, with the 1D $^1$H and $^{13}$C NMR spectra along the top and the side, respectively.

**Table 1.**

Chemical shifts of $^1$H and $^{13}$C NMR of $\beta$-CD unit in conjugate **23**.

| $^1$H NMR (ppm) | | $^{13}$C NMR (ppm) | |
|---|---|---|---|
| CD-$H_1$ | 5.64 | CD-$C_1$ | 96.29 |
| CD-$H_2$ | 4.73 | CD-$C_2$ | 69.81 |
| CD-$H_3$ | 5.34 | CD-$C_3$ | 70.67 |
| CD-$H_4$ | 3.53 | CD-$C_4$ | 76.51 |

| | | | |
|---|---|---|---|
| CD-$H_5$ | 4.47 | CD-$C_5$ | 69.64 |
| CD-$H_6$ | 4.85, 4.75 | CD-$C_6$ | 49.97 |

*3.3 In vitro cytotoxicity of heptavalent β-CD-GA conjugates*

It has been reported that GA **2** and some of its derivatives are cytotoxic in cancer cells (Satomi et al., 2005; Lallemand et al., 2011). In this study, the cytotoxicity of heptavalent *β*-CD-GA conjugates **21-28** and **33-38** was first determined in MDCK cells using the CellTiter-Glo® luminescent cell viability assay. Decrease in viability of MDCK cells was observed in a dose-dependent manner upon treatment of PTX (Supplementary data Fig. S3). Treatment of cells with **2** for 48 h resulted in decreased viability to 82.8% for the 25 $\mu$M concentration and no viability for the 10 $\mu$M concentration, indicating that **2** had weak cytotoxicity to cells and agreed with previously reported results that **2** shows weak cytotoxicity to eight cancer cell lines with $IC_{50}$ values between 70.48-136.40 $\mu$M (Gao et al., 2014). For all the tested conjugates, except that **25** and **28** showed weak cytotoxicity to uninfected MDCK cells with the reduced viability to 85.6% and 87.9%, respectively, at high concentration of 25 $\mu$M, no significant cytotoxicity for the other conjugates was observed at concentrations of 10 $\mu$M and 25 $\mu$M.

*3.4 Structure-activity relationships (SAR) of heptavalent β-CD-GA conjugates*

Concerning the fact that the use of multivalent sialopeptides as potential inhibitors of influenza infections has been proved to be a useful approach (Mammen et al., 1998; Marra et al., 2008), our interest was aimed at evaluating the inhibitory effect of the heptavalent GA conjugates **21-28** and **33-38** by microscopic examination of the viral CPE at 2 days post infection (Noah et al., 2007). Oseltamivir (OSV) and DMSO were used as positive and negative controls, respectively.

The primarily screening results are shown in Fig. 4. A careful analysis and comparison of the data allowed us to reveal some interesting SAR trends. Regarding the OEG linkers between the triazole ring substituted GA and *β*-CD scaffold, we found that the anti-influenza activity of conjugates **21-24** was decreased in the order as follows: **21**>**22**>>**23**>**24**. Similar results were also observed for conjugates **25-28**, indicating that a length of four atoms was found to be optimal for the inhibitory activity (**21** and **25**). Especially for conjugate **28**, the inserting of two more ethylene glycols spacer in **26** resulted in the loss of activity under 25 $\mu$M, suggesting the importance of the length of the linker between GA and *β*-CD for their anti-influenza activity. Concerning the nature of the linker's heteroatom, the replacement of the oxygen of ethylene glycol in conjugates **21** and **25** by methylene (**33** and **34**) showed slightly weaker or similar antiviral activity. Interesting, the increasing of the rigidity of the linker by further replacement of the four methylene with aromatic

benzene at positions at 1,4 (**35** and **36**) still retained reasonable anti-influenza activity. Surprisingly, the inserting of a piperazine space in the alkyl liner caused a substantial increase in activity of conjugates **37** and **38** (relative to **33** and **34**, respectively), which were proved to be the most two potent multivalent conjugates.

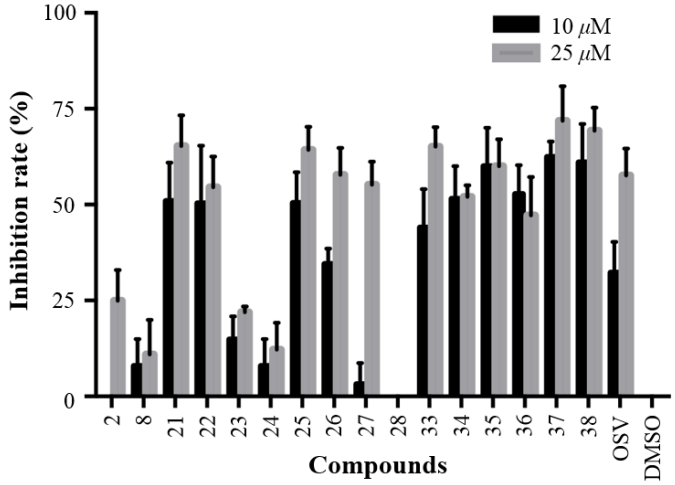


**Figure 4.** The CPE-based primarily screening of GA (**2**), *β*-CD (**8**) and their heptavalent *β*-CD-GA conjugates **21-28** and **33-38**. MDCK cells were utilized as the host cells to test A/WSN/33 virus infection; OSV and DMSO acted as positive and negative control, respectively. Error bars indicate standard deviations of triplicate experiments.

After the preliminary screening at two concentrations of 10 $\mu$M and 25 $\mu$M, 11 conjugates (**21-22**, **25-27** and **33-38**) with the inhibition rate over 50% at concentration of 25 μM were selected to perform in dose response assays, and the concentrations required to inhibit viral replication by 50% ($IC_{50}$) are summarized in Table 2. In addition, no significant toxicity was observed for the 10 conjugates at concentrations up to 100 $\mu$M. Based on these data, we investigated in detail the potential of a representative heptavalent conjugate **37**.

**Table 2.**

*In vitro* anti-influenza A virus activity of heptavalent conjugates **21-22**, **25-27** and **33-38**[a]

| Compd | $IC_{50}$, $\mu$M[b] | $CC_{50}$, $\mu$M | SI | Compd | $IC_{50}$, $\mu$M | $CC_{50}$, $\mu$M | SI |
|---|---|---|---|---|---|---|---|
| **2** | NA[c] | 85±6.8 | - | **33** | 12.1±0.31 | >100 | >8.3 |
| **8** | NA | ND[d] | - | **34** | 9.03±0.50 | >100 | >11.1 |
| **21** | 6.64±0.31 | >100 | >15.1 | **35** | 20.7±1.02 | >100 | >4.8 |
| **22** | 7.70±0.74 | >100 | >13.0 | **36** | 11.0±0.87 | >100 | >9.1 |
| **25** | 6.96±0.39 | >100 | >14.4 | **37** | 2.86±0.22 | >100 | >35.0 |
| **26** | 8.14±0.11 | >100 | >12.3 | **38** | 4.89±0.15 | >100 | >20.4 |

| | | | |
|---|---|---|---|
| **27** | 27.02±0.11 | >100 | >3.7 |

[a]Using influenza A/WSN/33 (H1N1) strain. [b]The concentration required for a test compound to reduce the virus-induced CPE by 50% relative to the virus control was expressed as $IC_{50}$. [c]No activity. [d]Not detectable.

The CPE produced by influenza A/WSN/33 virus in MDCK cells and its abrogation by treatment with **37** were further confirmed by direct observation under a microscope. No cytotoxicity was observed for **37** when incubated with the MDCK cells for 48 h (Supplementary data Fig. S4A *vs.* Fig. S4B), while **37** significantly reduced the CPE induced by influenza A/WSN/33 virus infection (Supplementary Fig. S4C *vs.* S4D).

*3.5 HI assay*

With the confirmation of the antiviral activity of the heptavalent conjugates, we were interested in identifying the molecular target of them. It is well known that the viral envelop glycoprotein HA plays a critical role in the initial step of influenza virus entry into host cells. Therefore, HI assay was designed to detect whether the heptavalent conjugates could interfere with the interaction between HA and its sialic acid receptors. Two fold dilutions of the heptavalent conjugate **37** (from 10 $\mu$M) or anti-HA antibody (from 0.50 ng/mL) treated virus were incubated with cRBC, and agglutination was observed (Fig. 5). In addition, **37** completely inhibited influenza A/WSN/33 (H1N1) virus induced agglutination of cRBC in a dose-dependent manner at concentrations of 1.3 $\mu$M or more. Similar results were observed for anti-HA antibody at concentrations of 0.063 ng/mL or more. These results suggested that the heptavalent conjugates **37** shared the same target of anti-HA antibody, thus interfering with virus-receptor interaction.

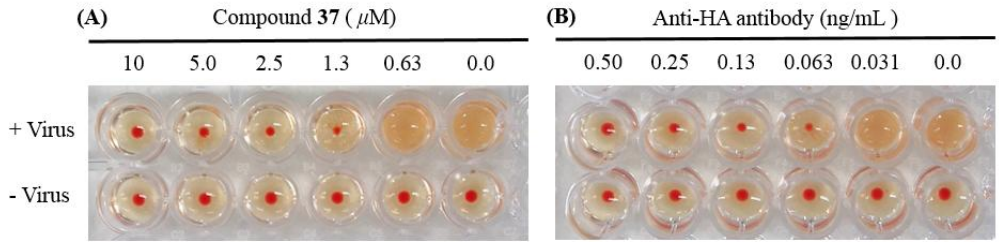


**Figure 5.** Effect of the heptavalent compound **37** (A) and anti-HA antibody (B) on HA by HI assay. The chicken red blood cells (cRBC) (1% v/v in saline) were incubated with influenza A/WSN/33 at 2 × HA with various concentrations of **37** (two-fold serial dilution from 10 $\mu$M) or anti-HA antibody (two-fold serial dilution from 0.50 ng/mL).

### *3.6 Determination of the $K_D$ for the interaction between the heptavalent conjugate **37** with HA protein*

To determine the binding affinity of conjugate **37** for the HA protein, SPR experiments were performed on a Biacore 8K instrument. The SPR response was reported in the resonance unites (RU). Sensor grams were analyzed with a 1:1 (Langmuir) binding mode. As shown in Fig. 6, the binding of recombinant influenza HA to GA (**2**) exhibited typical weak affinity binding with a calculated equilibrium dissociation constant ($K_D$) value of $2.45 \times 10^{-4}$ M, while $\beta$-CD (**8**) did not bind to HA protein at the same concentration. However, the multivalent conjugate **37** showed strong binding affinity to HA protein within the concentration range 0.16-5.00 $\mu$M. The calculated $K_D$ value for conjugate **37** was $5.15 \times 10^{-7}$ M, which seemed to be too large by about 470-fold of magnitude to that of **2** (Fig. 6A *vs.* Fig. 6C). In addition, kinetic analysis revealed that changes in multivalent conjugate and HA protein not only affected the association rate constant ($K_a$), but also affected the dissociation rate constant ($K_d$) (Supplementary data Table S1).

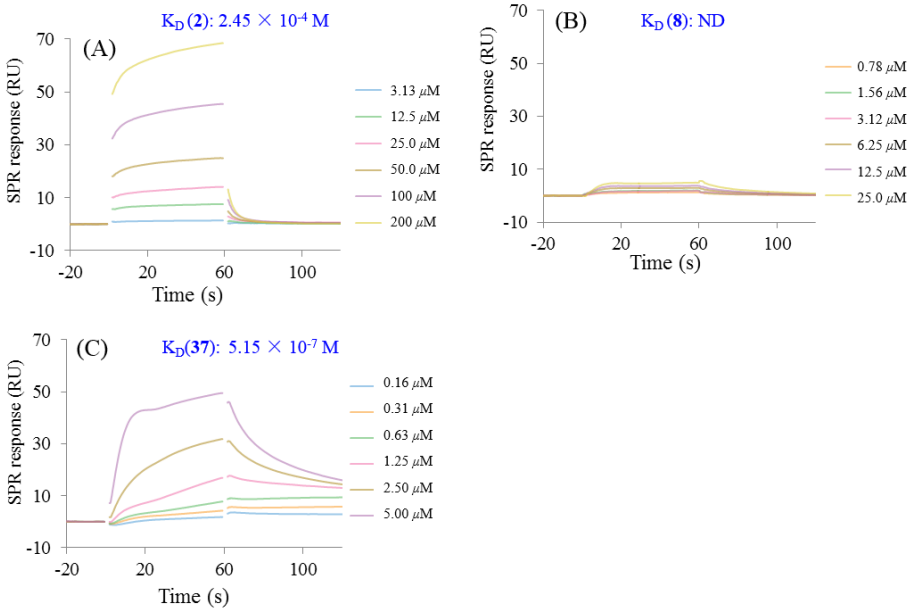


**Figure 6.** SPR inhibition assay sensor grams showing response to influenza HA protein in the presence of varying concentration of GA (**2**), $\beta$-CD (**8**) and their heptavalent conjugates **37**. The binding kinetics was analyzed by BIA evaluation 1.0.5 software with 1:1 (Langmuir) binding mode.

Compared with our previous study in which multiple pentacyclic triterpenes attached directly on CD scaffold via 1,2,3-triazolyl group (Xiao et al., 2016), the insertion of a suitable linker between them will helpful for the binding of multiple pentacyclic triterpenes with their target. To test the feasibility of the strategy, various types of linkers including flexible linear alkyl/ether chains combinations between 4 and 19 atoms, rigid aromatic space chain as well as semi-rigid charged piperzine chain have been successfully introduced in monovalent $\beta$-CD-GA conjugates in our recently study (Liang et al., 2019), which allowed us to further design and synthesis of the

second-generation multivalent pentacyclic triterpene-$\beta$-CD conjugates. This well-established method will provide an alternative approach to the construction of novel multivalent derivatives bearing different linkers based on natural or chemically modified CDs scaffolds. Combined with our previous studies, we found that the pentacyclic triterpenes pharmacophore, the CD scaffold and the linkers between the two parts were all affected their anti-influenza activity.

## 4. CONCLUSIONS

In this work, a series of multiple GA functionalized $\beta$-CD conjugates with different linkers were synthesized and characterized. Except that two conjugates (**25** and **28**) showed weak cytotoxicity to MDCK cells at concentration of 25 $\mu$M, all other conjugates showed no significant cytotoxicity based on an alamarBlue assay. When presented multivalently, seven $\beta$-CD-GA conjugates (**21**, **22**, **25**, **26**, **34**, **37** and **38**) showed strong anti-influenza properties with $IC_{50}$ values at a micromolar level ($IC_{50}$: 2.86-9.03 $\mu$M). By using of HI and SPR assays, conjugate **37** showed specific binding to HA protein with $K_D$ value at 515 nM, which was about 470-fold potent to its parent compound GA (**2**). Taken together, the results reported here for multivalent $\beta$-CD-GA conjugates demonstrated that multivalent displays of anti-influenza entry agent afford macromolecules with a remarkable activity and a strong binding to HA protein relative to their parent compound alone and multivalency based on $\beta$-CD scaffold is a promising alternative to the current available treatments for the management of viral infection by blocking virus entry into host cells.

## DATA AVAILABILITY STATEMENT

The raw data supporting the conclusions of this article will be made available by the authors, without undue reservation.

## AUTHOR CONTRIBUTIONS

SL and XM: design, synthesis and characterization of the multivalent conjugates; ML and YC: contribution in anti-influenza viral assay, HI assay,cytotoxicity assay; QG: SPR assay; YZ: discussion of all the experiments and assist in writing the manuscript; and LZ, DZ and SX: designed the synthesis and biochemical experiments, supervised the project, and wrote the manuscript.

## FUNDING

This work was supported by the International Cooperation and Exchange Program (NSFC-RFBR, No. 82161148006), the National Natural Science Foundation of China (Nos. 21877007 and 81821004) and Shenzhen Bay Laboratory Start-up Fundation (21230071).

## ACKNOWLEDGMENTS

The authors would like to thank Dr. Lijun Zhong from the Centre of Medical and Health Analysis (PUHSC) for MALDI-TOF experiments. The authors would also like to thank Dr. Fen Liu and Dr Jing Wang from State Key Laboratory of Natural and Biomimetic Drugs (PUHSC) for their help in conducting the NMR and SPR experiments, respectively.

## REFERENCES

Ashton, P. R., Koniger, R., Stoddart, J. F., Alker, D., Harding, V. D. (1996). Amino acid derivatives of *β*-cyclodextrin. *J. Org. Chem.* 61, 903-908. doi: 10.1021/Jo951396d

Asl, M. N., Hosseinzadeh, H. (2008). Review of pharmacological effects of Glycyrrhiza sp and its bioactive compounds. *Phytother. Res.* 22, 709-724. doi: 10.1002/ptr.2362

Chaudhary, P. M., Toraskar, S., Yadav, R., Hande, A., Yellin, R. A., Kikkeri, R. (2019). Multivalent sialosides: A tool to explore the role of sialic acids in biological processes. *Chem. Asian J.* 14, 1344-1355. doi: 10.1002/asia.201900031

Crini, G. (2014). Review: A history of cyclodextrins. *Chem. Rev.* 114, 10940-10975. doi: 10.1021/cr500081p

Das, K. (2012). Antivirals targeting influenza A virus. *J. Med. Chem.* 55, 6263-6277. doi: 10.1021/jm300455c

Fiore, C., Eisenhut, M., Ragazzi, E., Zanchin, G., Armanini, D. (2005). A history of the therapeutic use of liquorice in Europe. *J. Ethnopharmacol.* 99, 317-324. doi: 10.1016/j.jep.20005.04.015

Gadelle, A., Defaye, J. (1991). Selective halogenation at primary positions of cyclomaltooligosaccharides and a synthesis of per-3,6-anhydro cyclomaltooligosaccharides. *Angew. Chem. Int. Ed.* 30, 78-80. doi: 10.1002/anie.199100781

Gao, C., Dai, F. J., Cui, H. W., Peng, S. H., He, Y., Wang, X., et al. (2014). Synthesis of novel heterocyclic ring-fused 18β-glycyrrhetinic acid derivatives with antitumor and antimetastatic activity. *Chem. Biol. Drug Des.* 84, 223-233. doi: 10.1111/cbdd.12308

Gomez-Garcia, M., Benito, J. M., Butera, A. P., Mellet, C. O., Fernandez, J. M. G., Blanco, J. L. J. (2012). Probing carbohydrate-lectin recognition in heterogeneous environments with monodisperse cyclodextrin-based glycoclusters. *J. Org. Chem.* 77, 1273-1288. doi: 10.1021/jo201797b

Gomez-Garcia, M., Benito, J. M., Rodriguez-Lucena, D., Yu, J. X., Chmurski, K., Mellet, C. O., et al. (2005). Probing secondary carbohydrate-protein interactions with highly dense cyclodextrin-centered heteroglycoclusters: The heterocluster effect. *J. Am. Chem. Soc.* 127, 7970-7971. doi: 10.1021/ja050934t

Gonzalez-Gaitano, G., Isasi, J. R., Velaz, I., Zornoza, A. (2017). Drug carrier systems based on cyclodextrin supramolecular assemblies and polymers: Present and perspectives. *Curr. Pharm. Design* 23, 411-432. doi: 10.2174/1381612823666161118145309

Hardy, M. E., Hendricks, J. M., Paulson, J. M., Faunce, N. R. (2012). 18β-glycyrrhetinic acid inhibits rotavirus replication in culture. *Virol J* 9, 96. doi: 10.1186/1743-422x-9-96

Heo, Y. A. (2018). Baloxavir: First global approval. *Drugs* 78, 693-697. doi: 10.1007/s40265-018-0899-1

Hurt, A. C. (2014). The epidemiology and spread of drug resistant human influenza viruses. *Curr. Opin. Virol.* 8, 22-29. doi: 10.1016/j.coviro.2014.04.009

Hurt, A. C., Ho, H. T., Barr, I. (2006). Resistance to anti influenza drugs: Adamantanes and neuraminidase inhibitors. *Expert Rev. Anti-infect. Ther.* 4, 795-805. doi: 10.1586/14787210.4.5.795

Hussain, H., Green, I. R., Shamraiz, U., Saleem, M., Badshah, A., Abbas, G., et al. (2018). Therapeutic potential of glycyrrhetinic acids: A patent review (2010-2017). *Expert Opin. Ther. Pat.* 28, 383-398. doi: 10.1080/13543776.2018.1455828

Jansook, P., Ogawa, N., Loftsson, T. (2018). Cyclodextrins: structure, physicochemical properties and pharmaceutical applications. *Int. J. Pharmacol.* 535, 272-284. doi: 10.1016/j.ijpharm.2017.11.018

Karginov, V. A., Yohannes, A., Robinson, T. M., Fahmi, N. E., Alibek, K., Hecht, S. M. (2006). β-Cyclodextrin derivatives that inhibit anthrax lethal toxin. *Bioorg. Med. Chem.* 14, 33-40. doi: 10.1016/j.bmc.2005.07.054

Khan, A. R., Forgo, P., Stine, K. J., D'Souza, V. T. (1998). Methods for selective modifications of cyclodextrins. *Chem. Rev.* 98, 1977-1996. doi: 10.1021/Cr970012b

Kim, T. H., Yu, J. H., Jun, H., Yang, M. Y., Yang, M. J., Cho, J. W., et al. (2017). Polyglycerolated nanocarriers with increased ligand multivalency for enhanced in vivo therapeutic efficacy of paclitaxel. *Biomaterials* 145, 223-232. doi: 10.1016/j.biomaterials.2017.08.042

Lagacé-Wiens, P. R. S., Rubinstein, E., Gumel, A. (2010). Influenza epidemiology—past, present, and future. *Crit. Care Med.* 38, e1-e9. doi: 10.1097/CCM.0b013e3181cbaf34

Lallemand, B., Chaix, F., Bury, M., Bruyere, C., Ghostin, J., Becker, J. P., et al. (2011). *N*-(2-{3-[3,5-Bis(trifluoromethyl)phenyl]ureido}ethyl)-glycyrrhetinamide (6b): A novel anticancer glycyrrhetinic acid derivative that targets the proteasome and displays anti-kinase activity. *J. Med. Chem.* 54, 6501-6513. doi: 10.1021/jm200285z

Lepage, M. L., Schneider, J. P., Bodlenner, A., Compain, P. (2015). Toward a molecular lego approach for the diversity-oriented synthesis of cyclodextrin analogues designed as scaffolds for multivalent systems. *J. Org. Chem.* 80, 10719-10733. doi: 10.1021/acs.joc.5b01938

Leser, G. P., Lamb, R. A. (2005). Influenza virus assembly and budding in raft-derived microdomains: A quantitative analysis of the surface distribution of HA, NA and M2 proteins. *Virology* 342, 215-227. doi: 10.1016/j.virol.2005.09.049

Liang, S., Li, M., Yu, X., Jin, H., Zhang, Y., Zhang, L., et al. (2019). Synthesis and structure-activity relationship studies of water-soluble *β*-cyclodextrin-glycyrrhetinic acid conjugates as potential anti-influenza virus agents. *Eur. J. Med. Chem.* 166, 328-338. doi: 10.1016/j.ejmech.2019.01.074

Lin, J. C., Cherng, J. M., Hung, M. S., Baltina, L. A., Baltina, L., Kondratenko, R. (2008). Inhibitory effects of some derivatives of glycyrrhizic acid against Epstein-Barr virus infection: Structure-activity relationships. *Antiviral Res.* 79, 6-11. doi: 10.1016/j.antiviral.2008.01.160

Lu, W., Pieters, R. J. (2019). Carbohydrate–protein interactions and multivalency: Implications for the inhibition of influenza A virus infections. *Expert Opin. Drug Discov.* 14, 387-395. doi: 10.1080/17460441.2019.1573813

Mammen, M., Choi, S. K., Whitesides, G. M. (1998). Polyvalent interactions in biological systems: Implications for design and use of multivalent ligands and inhibitors. *Angew. Chem. Int. Ed.* 37, 2755-2794. doi: 10.1002/(SICI)1521-3773(19981102)37:20<2754::AID-ANIE2754>3.0.CO;2-3

Marra, A., Moni, L., Pazzi, D., Corallini, A., Bridi, D., Dondoni, A. (2008). Synthesis of sialoclusters appended to calix[4]arene platforms via multiple azide-alkyne cycloaddition. New inhibitors of hemagglutination and cytopathic effect mediated by BK and influenza A viruses. *Org. Biomol. Chem.* 6, 1396-1409. doi: 10.1039/b800598b

Martinez, A., Mellet, C. O., Fernandez, J. M. G. (2013). Cyclodextrin-based multivalent glycodisplays: covalent and supramolecular conjugates to assess carbohydrate-protein interactions. *Chem. Soc. Rev.* 42, 4746-4773. doi: 10.1039/c2cs35424a

Murelli, R. P., Zhang, A. X., Michel, J., Jorgensen, W. L., Spiegel, D. A. (2009). Chemical control over immune recognition: A class of antibody-recruiting small molecules that target prostate cancer. *J. Am. Chem. Soc.* 131, 17090-17092. doi: 10.1021/ja906844e

Neumann, G., Noda, T., Kawaoka, Y. (2009). Emergence and pandemic potential of swine-origin H1N1 influenza virus. *Nature* 459, 931-939. doi: 10.1038/nature08157

Noah, J. W., Severson, W., Noah, D. L., Rasmussen, L., White, E. L., Jonsson, C. B. (2007). A cell-based luminescence assay is effective for high-throughput screening of potential influenza antivirals. *Antiviral Res.* 73, 50-59. doi: 10.1016/j.antiviral.2006.07.006

Ortega-Caballero, F., Gimenez-Martinez, J. J., Garcia-Fuentes, L., Ortiz-Salmeron, E., Santoyo-Gonzalez, F., Vargas-Berenguel, A. (2001). Binding affinity properties of dendritic glycosides based on a β-cyclodextrin core toward guest molecules and concanavalin A. *J. Org. Chem.* 66, 7786-7795. doi: 10.1021/jo015875q

Rao, C. N. R., Venkataraghavan, R. (1964). Contribution to infrared spectra of five-membered *N*- and *N,S*-heterocyclic compounds. *Can. J. Chem.* 42, 43-49. doi: 10.1139/V64-007
Sanhueza, C. A., Baksh, M. M., Thuma, B., Roy, M. D., Dutta, S., Preville, C., et al. (2017). Efficient liver targeting by polyvalent display of a compact ligand for the asialoglycoprotein receptor. *J. Am. Chem. Soc.* 139, 3528-3536. doi: 10.1021/jacs.6b12964
Satomi, Y., Nishino, H., Shibata, S. (2005). Glycyrrhetinic acid and related compounds induce G1 arrest and apoptosis in human hepatocellular carcinoma HepG2. *Anticancer Res.* 25, 4043-4047. doi:
Sauter, N. K., Bednarski, M. D., Wurzburg, B. A., Hanson, J. E., Whitesides, G. M., Skehel, J. J., et al. (1989). Hemagglutinins from 2 influenza-virus variants bind to sialic-acid derivatives with millimolar dissociation-constants: A 500-MHz proton nuclear magnetic-resonance study. *Biochemistry* 28, 8388-8396. doi: 10.1021/Bi00447a018
Schwarz, S., Lucas, S. D., Sommerwerk, S., Csuk, R. (2014). Amino derivatives of glycyrrhetinic acid as potential inhibitors of cholinesterases. *Bioorg. Med. Chem.* 22, 3370-3378. doi: 10.1016/j.bmc.2014.04.046
Si, L. L., Meng, K., Tian, Z. Y., Sun, J. Q., Li, H. Q., Zhang, Z. W., et al. (2018). Triterpenoids manipulate a broad range of virus-host fusion via wrapping the HR2 domain prevalent in viral envelopes. *Sci. Adv.* 4, eaau8408. doi: 10.1126/sciadv.aau8408
Skehel, J. J., Wiley, D. C. (2000). Receptor binding and membrane fusion in virus entry: The influenza hemagglutinin. *Annu. Rev. Biochem.* 69, 531-569. doi: 10.1146/annurev.biochem.69.1.531
Stanetty, C., Wolkerstorfer, A., Amer, H., Hofinger, A., Jordis, U., Classen-Houben, D., et al. (2012). Synthesis and antiviral activities of spacer-linked 1-thioglucuronide analogues of glycyrrhizin. *Beilstein J. Org. Chem.* 8, 705-711. doi: 10.3762/bjoc.8.79
Tran, F., Odell, A. V., Ward, G. E., Westwood, N. J. (2013). A modular approach to triazole-containing chemical inducers of dimerisation for yeast three-hybrid screening. *Molecules* 18, 11639-11657. doi: 10.3390/molecules180911639
van der Vries, E., Stelma, F. F., Boucher, C. A. B. (2010). Emergence of a multidrug-resistant pandemic influenza A (H1N1) virus. *New Engl. J. Med.* 363, 1381-1382. doi: 10.1056/Nejmc1003749
van Dongen, M. J. P., Kadam, R. U., Juraszek, J., Lawson, E., Brandenburg, B., Schmitz, F., et al. (2019). A small-molecule fusion inhibitor of influenza virus is orally active in mice. *Science* 363, eaar6221. doi: 10.1126/science.aar6221
Vargas-Berenguel, A., Ortega-Caballero, F., Santoyo-Gonzalez, F., Garcia-Lopez, J. J., Gimenez-Martinez, J. J., Garcia-Fuentes, L., et al. (2002). Dendritic galactosides based on a β-cyclodextrin core for the construction of site-specific molecular delivery systems: Synthesis and molecular recognition studies. *Chem-Eur J* 8, 812-827. doi: 10.1002/1521-3765(20020215)8:4<812::Aid-Chem812>3.0.Co;2-P
Wang, L. J., Geng, C. A., Ma, Y. B., Huang, X. Y., Luo, J., Chen, H., et al. (2012). Synthesis, biological evaluation and structure-activity relationships of glycyrrhetinic acid derivatives as novel anti-hepatitis B virus agents. *Bioorg Med Chem Lett* 22, 3473-3479. doi: 10.1016/j.bmcl.2012.03.081
Xiao, S., Si, L., Tian, Z., Jiao, P., Fan, Z., Meng, K., et al. (2016). Pentacyclic triterpenes grafted on CD cores to interfere with influenza virus entry: A dramatic multivalent effect. *Biomaterials* 78, 74-85. doi: 10.1016/j.biomaterials.2015.11.034
Yang, R., Wang, L. Q., Yuan, B. C., Liu, Y. (2015). The pharmacological activities of licorice. *Planta Med* 81, 1654-1669. doi: 10.1055/s-0035-1557893
Yu, M., Si, L., Wang, Y., Wu, Y., Yu, F., Jiao, P., et al. (2014). Discovery of pentacyclic triterpenoids as potential entry inhibitors of influenza viruses. *J. Med. Chem.* 57, 10058-10071. doi: 10.1021/jm5014067
Zhang, A. X., Murelli, R. P., Barinka, C., Michel, J., Cocleaza, A., Jorgensen, W. L., et al. (2010). A remote arene-binding site on prostate specific membrane antigen revealed by antibody-recruiting small molecules. *J. Am. Chem. Soc.* 132, 12711-12716. doi: 10.1021/ja104591m
Zhang, Q., Li, G. Z., Becer, C. R., Haddleton, D. M. (2012). Cyclodextrin-centred star polymers synthesized via a combination of thiol-ene click and ring opening polymerization. *Chem. Commun.* 48, 8063-8065. doi: 10.1039/c2cc33742h
Zhou, L., Lv, F., Liu, L., Wang, S. (2019). In situ-induced multivalent anticancer drug clusters in cancer cells for enhancing drug efficacy. *CCS Chem.* 1, 97-105. doi: 10.31635/ccschem.019.20180015
Zigolo, M. A., Salinas, M., Alche, L., Baldessari, A., Linares, G. G. (2018). Chemoenzymatic synthesis of new derivatives of glycyrrhetinic acid with antiviral activity. Molecular docking study. *Bioorg. Chem.* 78, 210-219. doi: 10.1016/j.bioorg.2018.03.018